Crystallization of Poly(ethylene oxide) Confined in Miniemulsion Droplets

Andreas Taden and Katharina Landfester*

Max Planck Institute of Colloids and Interfaces, Research Campus Golm, 14424 Golm, Germany

Received January 16, 2003; Revised Manuscript Received April 4, 2003

ABSTRACT: Crystallization of the poly(ethylene oxide) (PEO) confined in narrowly distributed, stable nanodroplets with a size of about 100 nm as obtained by the miniemulsion process is analyzed using DSC measurements. It is shown that nucleation in these PEO droplets occurs only at large supercooling. It is found that the polymer structure in the crystallized droplets is topologically controlled. PEO forms loosely layered lamellar structure in the droplets. Drying of the dispersion leads to a highly ordered arrangement of PEO platelets of different sizes but a constant height of about 25 nm as detected by TEM and AFM.

Introduction

Crystallization processes are induced by either heterogeneous or homogeneous nucleation. Whereas heterogeneous nucleation occurs at a low supercooling of the material below the transition temperature, the supercooling required for homogeneous nucleation is usually much larger. Crystallization studies of polymer droplets were first published by Turnbull et al. in the 1960s.[1,2] The crystallization in restricted geometries shows that confinement affects the nucleation mechanism significantly, and a shift from heterogeneous to homogeneous nucleation is easily obtained. This is due to the fact that the few highly active heterogeneous nuclei which could be active in a bulk system are now distributed in only some of the formed compartments whereas most of them are free of such heterogeneous nuclei.[3−5] Each of these compartments has then to nucleate homogeneously at larger supercooling in order to start crystallization in each compartment individually. The difference in the crystallization temperature between heterogeneous and homogeneous nucleation can already lead to different crystal morphologies. A different crystallization behavior is also obtained by the confinement itself which restricts the number of possible conformations and reduces the number of available molecules, as it was recently shown for even alkanes (C18 to C24). Here a structure change from the triclinic in the bulk to orthorhombic structure in small droplets (100 nm) was detected.[6]

Compared to low molecular weight material, the situation of polymers in confined systems is even more complex since already the transition in bulk from amorphous, randomly coiled state of polymers into a crystalline, ordered lamellar state is still far away from being understood.[7] The formation of the initial nuclei,[8,9] the growth kinetics resulting in folded intermediate metastable states,[10,11] and the morphology evolution during annealing[12,13] are discussed controversially in many papers. Recently, crystallization of polymers in restricted areas was studied by several groups in order to get more information about the ordering process. Arnal et al. reported on crystallizable polymers like isotactic polypropylene (PP) or linear low-density polyethylene (LDPE) which were dispersed in an incompatible matrix like atactic polystyrene with domain sizes up to several micrometers.[14,15] They observed a fractionated crystallization if the number of dispersed droplets was greater than the number of active heterogeneities originally present in the bulk polymer. The fractionated crystallization was attributed to the fact that the droplets which contain the heterogeneous nuclei nucleate at low supercooling; the droplets without these heterogeneities will only nucleate at larger supercooling needed to generate homogeneous nucleation.

With decreasing average droplet size and therefore increasing number of droplets, a decreasing percentage of the PP droplets still contain the heterogeneous nuclei whereas most of the PP droplets show the remarkable decrease of the crystallization temperatures of up to 64 K. This low crystallization temperature is very close to the homogeneous nucleation temperature of linear polyolefins.

Crystallization in much smaller domains was observed in block copolymer systems. Because of small domain sizes, the nucleation mechanism could be shifted entirely to homogeneous nucleation. In many cases, PEO represents the crystallizing block; e.g., Ryan et al. investigated the crystallization on PEO-*b*-PBO (poly(butylene oxide)),[16] and Cheng et al. studied the behavior in the PEO-*b*-PS system.[17,18]

In a hydrogenated PB−PEO system (where PB is polybutadiene (please note that hydrogenated PB is equivalent to poly(butylene-*co*-ethylene)) as presented by Reiter et al.,[19] the crystallization of 12 nm PEO spheres was characterized. By cooling the sample, all PEO spheres crystallized individually and independently. Melting of the confined crystals was also a stochastical process where not all spheres melted at the same temperature, indicating different degrees of order of the individual small crystals. The disadvantage of the block copolymer system is that the crystallizing PEO block is fixed to the interface, and free crystallization of the chains is prohibited. This is why miniemulsion droplets consisting of homopolymer may add additional information on crystallization behavior.

In this contribution, we want to employ a new model system for the examination of the crystallization of poly(ethylene oxide) in narrowly distributed nanodroplets. The size of the droplets should be in the 100 nm range, which is expected to be small enough that only homogeneous nucleation takes place and large enough that

10.1021/ma034052v CCC: $25.00

Table 1. Characteristics of the PEO Dispersions

polymer	sample	particle diameter [nm]	std dev	$T_m{}^a$ [°C]	$T_c{}^a$ [°C]	melting hysteresis T_m-T_c
PEO 8600	miniemulsion	83	0.33	59.8	−23.3	83.1
	bulk			62.0	42.8	19.2
PEO 12000	miniemulsion	83	0.33	57.7	−23.9	81.6
	bulk			62.7	43.0	19.7
PEO 40000	miniemulsion	120	0.21	61.8	−20.5	82.3
	bulk			65.3	47.0	18.3
PB/E−PEO	bulk			56.0	39.7	16.3

[a] Melting temperature. [b] Crystallization temperature.

a crystal superstructure of the polymer can be detected. Since lamellar structures of polymers are in the region of 20−25 nm, the size of the droplet is expected to have a strong influence on the structure. These small nanodroplets are obtained by the miniemulsion process.[20,21] Miniemulsions provide small, stable, and narrowly distributed nanodroplets with a controllable size in the range 50−500 nm. Their highly reproducible generation by high shear devices, the stabilization by combination of surfactants and osmotic pressure controlling agents, and some of their properties were recently reviewed and are not discussed here in detail.[22] The aim of this paper is to investigate the differences between the crystallization process of poly(ethylene oxide) in small miniemulsion droplets in comparison to the bulk material.

Experimental Part

Materials. Poly(ethylene oxide) standard 8600 ($M_w = 8350$ g mol^{-1}, $D = 1.03$), poly(ethylene oxide) standard 12000 ($M_w = 11\,600$ g mol^{-1}, $D = 1.04$), and poly(ethylene oxide) standard 40000 ($M_w = 41\,500$ g mol^{-1}, $D = 1.14$) from Fluka were used as received. The block copolymer emulsifier poly(butylene-*co*-ethylene)-*b*-poly(ethylene oxide) P(B/E)−PEO consisting of a hydrophobic block ($M_w = 3700$ g mol^{-1}) and a hydrophilic block ($M_w = 3600$ g mol^{-1}) was synthesized starting from Kraton L (Shell) dissolved in toluene by adding ethylene oxide under the typical conditions of anionic polymerization.[23] Isopar M (an isoparaffinic hydrocarbon) was a gift from Exxon Chemical.

Preparation of the Inverse Miniemulsions. 300 mg of PEO was dissolved in 3.0 g of water and added to a solution of 150 mg of poly(butylene-*co*-ethylene)-*b*-poly(ethylene oxide) (P(B−E)/PEO) and 6.0 g of Isopar M. After stirring for 1 h, the miniemulsion was prepared by ultrasonicating the emulsion with a Branson sonifier W450 (microtip) at an amplitude of 70% (10 min overall ultrasonication time: 5 s pulsing/10 s waiting time). To prevent a temperature rise in the sample, the emulsion was ice-cooled. After sonication, the sample was heated overnight at 60 °C for the evaporation of the water.

Analytical Methods. The particle sizes were measured using a Nicomp particle sizer (model 370, PSS Santa Barbara, CA) at a fixed scattering angle of 90°.

The DSC measurements were carried out using a Netzsch Thermal Analyse DSC 200. The measurements were carried out in the scanning mode. Sample masses between 10 and 20 mg were used. For the measurement, the sample was heated to 75 °C, held at that temperature for 5 min, and then cooled to −55 °C. Cooling and heating rates of 5 K min^{-1} were used for all measurements.

Wide-angle X-ray (WAXS) diffraction was measured with a Nonius CP-120 diffractometer using Cu Kα radiation ($\lambda = 0.154$ nm). The measurements were performed at room temperature after crystallization of the PEO at lower temperatures (as verified by DSC).

Transmission electron microscopy was performed with a Zeiss 912 Omega electron microscope operating at 100 kV. The diluted samples were mounted on 400 mesh carbon-coated copper grids and left to dry. Contrasting was not applied.

Scanning force microscopy (AFM) was performed with a NanoScope IIIa microscope (Digital Instruments, Santa Barbara, CA) operating in tapping mode. The instrument was equipped with a 10×10 μm E-Scanner and commercial silicon tips (model TSEP; the force constant was 50 N m^{-1}, the resonance frequency was 300 kHz, and the tip radius was smaller than 20 nm). The height, amplitude, and phase signal were monitored. The samples were prepared by letting droplets of diluted aqueous solution (0.05 wt %) dry on freshly cleaved muscovite mica surfaces at room temperature.

Results and Discussion

Stable miniemulsions consisting of narrowly size distributed PEO particles with PEO of different molecular weight were obtained in an inverse miniemulsion process. The inverse miniemulsions were prepared by dispersing aqueous PEO solutions in Isopar M using P(B/E)−PEO as surfactant. Then the water was removed by evaporation at 60 °C in order to obtain pure PEO droplets. The characteristics of the PEO miniemulsions with PEO 8600, 12000, and 40000 are summarized in Table 1.

DSC measurements were used to investigate the dynamical crystallization temperature of the poly(ethylene oxide). It is important to note that the continuous phase, the Isopar M, is not frozen under the measurement conditions (cooling until −55 °C).

Figure 1a shows the DSC curves for PEO 8600 in bulk and in miniemulsion with a mean droplet size of 83 nm. Heating the samples with crystallized droplets results in a decrease of the (dynamic) melting point in droplets of 2.2 °C from 62.0 to 59.8 °C. Whereas in the bulk material the crystallization and the melting enthalpy correspond to each other ($-\Delta H_{\text{cryst}} \approx \Delta H_{\text{melt}}$), it is obviously not the case in the miniemulsion. Here, the change of the crystallization enthalpy is about 60% of the melting enthalpy, which can be attributed to structural imperfections of the crystals due to fast cooling process. Since a complete stretching of the polymer chains is hindered and only a metastable state is formed, crystalline and amorphous superstructures may coexist. At the following heating, a reorganization of the material can take place, leading to a crystal perfection which leads to a larger melting peak as also recently reported by Thurn-Albrecht et al.[24]

The temperature at which (dynamic) crystallization of the PEO in the miniemulsion occurs is much lower than in bulk PEO; it was strongly shifted from 42.8 °C in bulk to about −23.3 °C in miniemulsion. Therefore, the melting hysteresis (T_m-T_c) in the miniemulsion droplets increases to more than 80 °C, and the droplets are usually still liquid at room temperature. The dynamic crystallization of the polymer in the droplets is much more influenced than the melting process. As was recently shown, the low crystallization temperature is not due to the thermodynamics in small miniemulsion droplets and is also not affected by the surfactant on the droplet surface.[5,6] This indicates that, in analogy to low M_w components as shown recently,[5] the nucleation

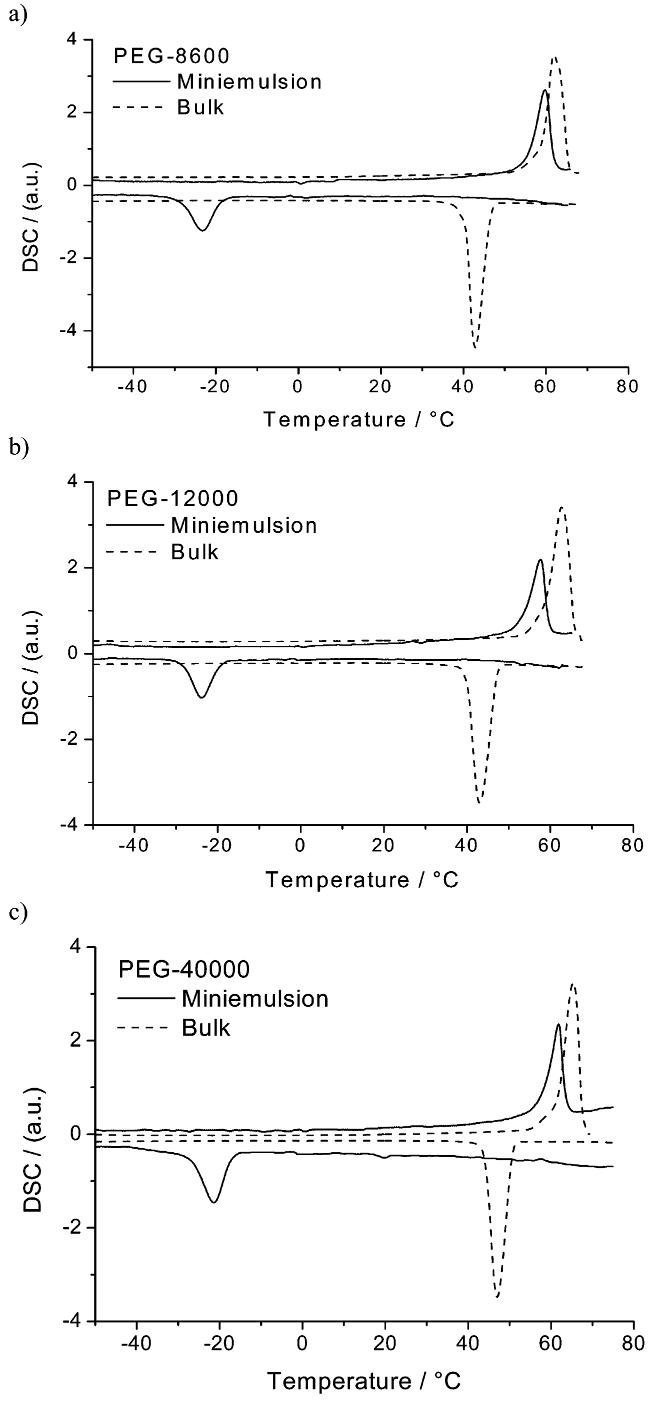

Figure 1. Comparison PEO as bulk and as droplets in miniemulsion. Cooling and heating rates: 5 K min^{-1}. (a) PEO 8600; (b) PEO 12000; (c) PEO 40000.

of all droplets is indeed shifted from heterogeneous to homogeneous nucleation since the few highly active heterogeneous nuclei which could be active in a bulk system are distributed in only some of the formed compartments. The amount of those droplets is that low that they remain unseen by DSC measurement. The hysteresis corresponds very well with values reported for homogeneous nucleation of PEO in very small (12 nm) confinement.[19] The remaining small differences are explained by the very weak dependence of the crystallization on the droplet size.[5]

Contrary to the blend systems where fractionated crystallization was found,[25] in miniemulsions crystallization occurs only at one temperature. The difference is due to the fact that in the miniemulsion the droplets are much smaller (100 nm) with a narrow size distribution.

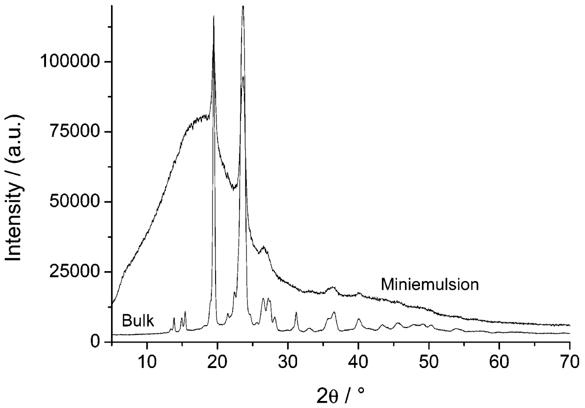

Figure 2. WAXS of dispersion PEO 12000 and the correspondent bulk system.

It has also to be noted that the miniemulsion droplets are stabilized by the diblock copolymer PB/E-PEO and that the PEO chains of the surfactants with a molecular weight of 3600 g mol^{-1} might also lead to an additional slight depression of the melting and crystallization temperature compared to the case of pure material.

In the next set of experiments, PEO of higher molecular weight was used for the formulation of the droplets. Using PEO 12000 and 40000, a slight increase of melting and crystallization temperature in the bulk system was detected (see Figure 1b and Table 1). However, a contrary effect is seen for the miniemulsion containing PEO 12000. With the same droplet size as in the case of PEO 8600, both the melting and the crystallization temperature are decreased. Because of the very large undercooling and the related higher viscosity, the crystallization in miniemulsion is kinetically more sensitive, and therefore longer chains are even more affected.

A further increase of the molecular weight to PEO 40000 increases in the bulk, and in the miniemulsion the melting and crystallization temperatures compared to those of the samples with lower molecular weight (see Figure 1c and Table 1).

Whereas DSC measurements just detect differences in the crystallization and melting temperature, the underlying structure remains unresolved. This is why we applied techniques for the characterization of the particles morphology. Wide-angle X-ray measurements have been used in order to analyze the crystals formed in bulk and under confined conditions in the nanodroplets. Figure 2 shows the X-ray diffraction at room temperature of the bulk PEO 12000 and the miniemulsion after crystallization of the droplets at low temperature. In the miniemulsion, beside a broad signal from the continuous phase Isopar M, strong peaks at 19.5° and 23.6° are detected without any shift compared to the case of the bulk system.

The crystallite sizes can be estimated from the line width of the WAXS peaks using the Scherrer equation. Evaluating the peak at 19.5°, crystallite sizes of about 30 nm for the bulk system and about 20 nm for the miniemulsion system were detected, sizes which can be attributed to formed lamellae. The difference of the sizes is due to the strong dependence of the characteristic length on the temperature as also shown for thin films by Reiter et al. The larger the undercooling and there-

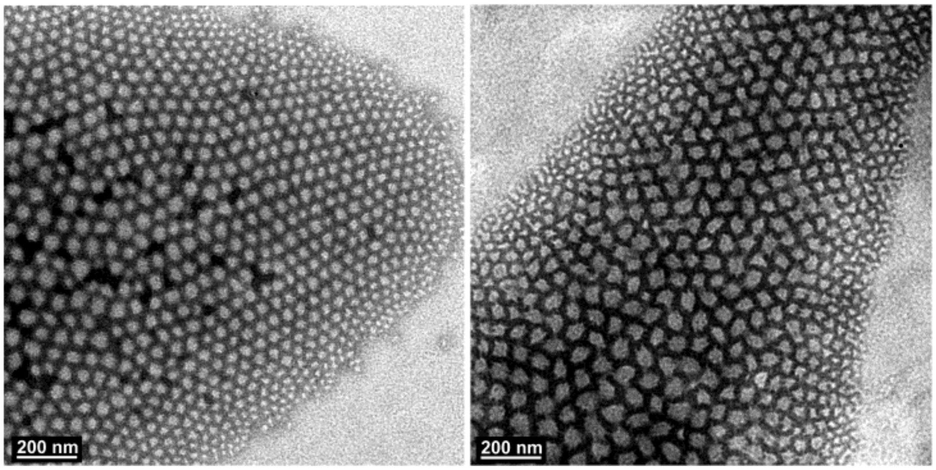

Figure 3. Electron micrograph obtained from the dispersion with PEO 12000.

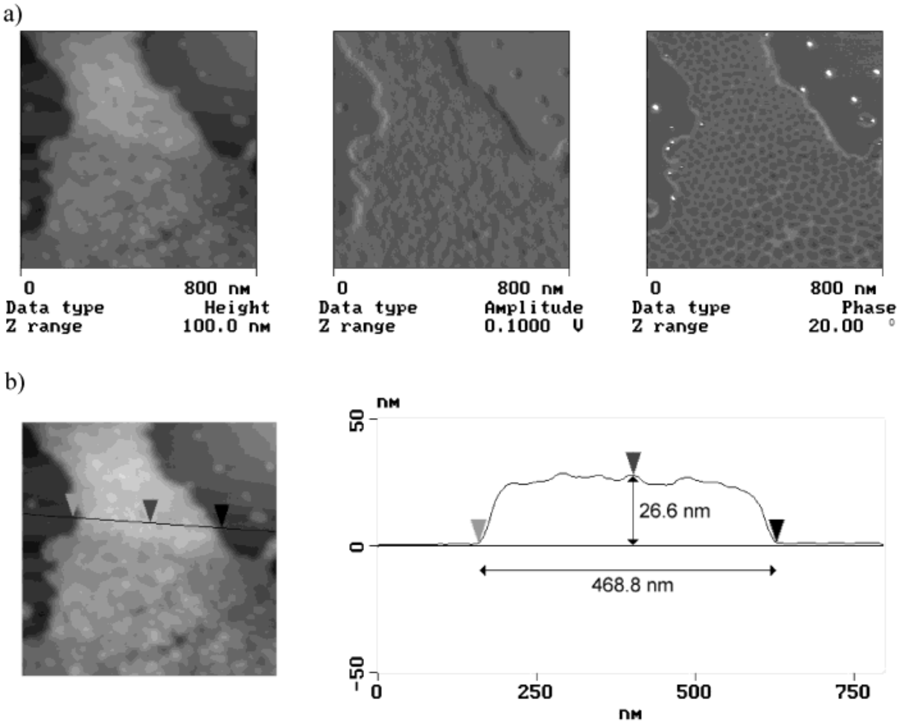

Figure 4. (a) AFM pictures of dispersion PEO 12000 and (b) a section analysis.

fore the faster the crystallization are, the higher is the tendency for chain folds.[26]

It is quite astonishing that, despite the crystallization inside the droplets, the size of the crystallized droplets does not change, and the dispersion remains stable. This means that no large deformation with increasing the interface (which had to be stabilized additionally) between the crystal and the dispersed phase takes places. Therefore, the formed polymer crystals indeed fit into the 100 nm droplets.

As a second method for the characterization of the structure, TEM analysis was used. Typical TEM pictures of sample PEO 12000 are shown in Figure 3. The white parts can be attributed to crystallized material, and the surrounding black parts represent the amorphous parts of the P(B/E)−PEO surfactant. The polyhedral units of different sizes between 90 and 10 nm arrange in a highly regular, but not periodic, way. The arrangement of the polyhedral units follows the rules of hyperbolic geometries. It is seen that the polyhedral units are not homogeneously distributed over the surface, but clusters of the polyhedral units are formed where the larger ones are at the inside and the smaller ones are located on the border. Such structures have also been observed for polymer latexes with a broad Gaussian distribution and are named “Zenon” packing following the fable of Achilles and the turtle that introduced the concept of hyperbolic borderlines into philosophy and science.[27] The size of the largest polyhedrons corresponds very well to the size of the droplets in dispersion as measured by light scattering. The smaller sizes (down to 10 nm) are not existent as small particles in dispersion, indicating that they are formed while film formation and drying. In AFM studies it is clearly seen (Figure 4) that the polyhedrons which arrange after drying, even though they have different sizes in the $x-y$ dimension (10−90 nm), are all platelet-like with a constant height of about 25 nm, a size which is again consistent to the height of PEO lamellae formed at low temperature.[26] This means that the PEO chains crystallize in single fold lamellar crystals, which are not interconnected with each other, indicating that an

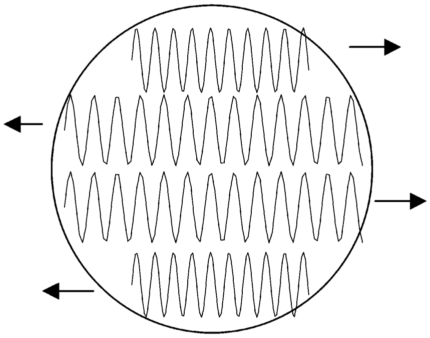

Figure 5. Scheme of the loosely packed PEO lamellae in the droplets which can slide apart while drying.

interlamellar crystallization of one PEO chain does not occur. Comparing the volume of the platelets, one can calculate that each of the original droplet consists of 4−5 of the polyhedral units (detected by TEM or AFM). These lamellae must have been formed by 4−5 individual nucleation processes. The formation does not occur simultaneously, but in succession. At one time in each of the droplets only one nucleus is present.

All these measurements lead to the conclusion that the PEO forms in average a pile of about 4−5 noninterconnected lamellae in each droplet. In dispersion, such a structure is fixed inside the droplets by the surface tension; however, upon drying of the dispersion the fragile structure allows a sliding of the lamellae (see Figure 5), resulting in platelets of constant height.

Conclusion

Crystallization of poly(ethylene oxide) in narrowly distributed nanodroplets as obtained by the miniemulsion approach was examined. The size of the droplets was chosen to be in the 100 nm range. It was shown that the small and narrowly size distributed droplets show exclusively homogeneous nucleation, resulting in stable crystallized droplets. Inside each droplet, 4−5 lamellae are formed which are not interlamellar connected and just loosely layered. During the crystallization, in each droplet, only one nucleus is present at the same time. At the large supercooling only about 60% of the chains are crystallized, indicating a high imperfection of the superstructure. However, a rearrangement occurs at increasing temperature. Whereas in dispersion the structure is stable, upon drying the lamellae slid apart from each other and arrange in a highly ordered, *Zenon*-structural way. The smallest units (the “cap” of the droplet) indeed consists of down to one polymer chain. Therefore, the crystallization of polymers confined in miniemulsion can be also used to obtain single chain single crystals.

Acknowledgment. We especially thank Markus Antonietti for helpful discussions. Ines Below is thanked for synthesizing the P(B/E)−PEO block copolymer.

References and Notes

(1) Cormia, R. L.; Price, F. P.; Turnbull, D. *J. Chem. Phys.* **1962**, *37*, 1333−1340.
(2) Burns, J. R.; Turnbull, D. *J. Appl. Phys.* **1966**, *37*, 4021−4026.
(3) Vonnegut, B. *J. Colloid Sci.* **1948**, *3*, 563.
(4) Kelton, K. F. *Solid State Phys.* **1991**, *45*, 75.
(5) Montenegro, R.; Antonietti, M.; Mastai, Y.; Landfester, K. *J. Chem. Phys.*, in press.
(6) Montenegro, R.; Landfester, K. *Langmuir*, in press.
(7) Strobl, G. *The Physics of Polymers*; Springer: Berlin, 1997.
(8) tenWolde, P. R.; Frenkel, D. *Science* **1997**, *277*, 1975.
(9) Liu, C.; Mutthukumar, M. *J. Chem. Phys.* **1998**, *109*, 2536.
(10) Keller, A.; Cheng, S. Z. D. *Polymer* **1998**, *39*, 4461.
(11) Doye, J. P. K.; Frenkel, D. *Phys. Rev. Lett.* **1998**, *81*, 2160.
(12) Reiter, G.; Castelein, G.; Sommer, J.-U. *Phys. Rev. Lett.* **2001**, *86*, 5918.
(13) Zhou, W.; Cheng, S. Z. D.; Putthanarat, S.; Eby, R. K.; Reneker, D. H.; Lotz, B.; Magonov, S.; Hsieh, E. T.; Geerts, R. G.; Palackal, S. P.; Hawley, G. R.; Welch, M. B. *Macromolecules* **2000**, *33*, 6861−6868.
(14) Arnal, M. L.; Matos, M. E.; Morales, R. A.; Santana, O. O.; Muller, A. J. *Macromol. Chem. Phys.* **1998**, *199*, 2275−2288.
(15) Arnal, M. L.; Muller, A. J. *Macromol. Chem. Phys.* **1999**, *200*, 2559−2576.
(16) Xu, J. T.; Fairclough, J. P. A.; Mai, S. M.; Ryan, A. J.; Chaibundit, C. *Macromolecules* **2002**, *35*, 6937−6945.
(17) Zhu, L.; Mimnaugh, B. R.; Ge, Q.; Quirk, R. P.; Cheng, S. Z. D.; Thomas, E. L.; Lotz, B.; Hsiao, B. S.; Yeh, F. J.; Liu, L. Z. *Polymer* **2001**, *42*, 9121−9131.
(18) Wang, S.; Dai, Q. P.; Hong, J. M.; Yang, X. H.; Cheng, R. S. *Chem. J. Chin. Univ.* **1998**, *19*, 1526−1528.
(19) Reiter, G.; Castelein, G.; Sommer, J.-U.; Röttele, A.; Thurn-Albrecht, T. *Phys. Rev. Lett.* **2001**, *87*, 6104−6104.
(20) Landfester, K. *Adv. Mater.* **2001**, *10*, 765−768.
(21) Antonietti, M.; Landfester, K. *Prog. Polym. Sci.* **2002**, *27*, 689−757.
(22) Landfester, K. *Macromol. Rapid Commun.* **2001**, *22*, 896−936.
(23) Schlaad, H.; Kukula, H.; Rudloff, J.; Below, I. *Macromolecules* **2001**, *34*, 4302−4304.
(24) Röttele, A.; Thurn-Albrecht, T.; Sommer, J.-U.; Reiter, G. *Macromolecules*, submitted for publication.
(25) Arnal, M. L.; Muller, A. J.; Maiti, P.; Hikosaka, M. *Macromol. Chem. Phys.* **2000**, *201*, 2493−2504.
(26) Reiter, G.; Castelein, G.; Sommer, J.-U. *Macromol. Symp.* **2002**, *183*, 173−178.
(27) Antonietti, M.; Hartmann, J.; Neese, M.; Seifert, U. *Langmuir* **2000**, *16*, 7634−7639.

MA034052V